Journal of Biotechnology 395 (2024) 1–11

Contents lists available at ScienceDirect

Journal of Biotechnology

journal homepage: www.elsevier.com/locate/jbiotec

# Advanced enzymatic multigram-scale production of nucleotide sugars in a continuous fed-batch membrane reactor

Hannes Frohnmeyer, Nikol Kodra, Lothar Elling *

*Laboratory for Biomaterials, Institute of Biotechnology, and Helmholtz-Institute for Biomedical Engineering, RWTH Aachen University, Pauwelsstraße 20, Aachen 52074, Germany*

ARTICLE INFO

*Keywords:*
Nucleotide sugars
Continuous production
Enzyme cascades
Gram-scale

ABSTRACT

Enzymatic production of nucleotide sugars on a multigram scale presents a challenge, as only a few processes have been reported for large-scale nucleotide sugar production. They rely primarily on batch synthesis and employ exceptional amounts of enzymes. This study introduces a novel approach for the multigram-scale production of nucleotide sugars with a continuous fed-batch membrane reactor. We successfully synthesized five main nucleotide sugars: UDP-Gal, UDP-GalNAc, UDP-GlcA, GDP-Man, and CMP-Neu5Ac on a multigram scale. Efficient biocatalyst utilization results in high performance, including space-time yield (STY, $g*L^{-1}h^{-1}$), total turnover number (TTN, g product per g enzyme), and an efficient product formation rate (g/h) suitable for industrially relevant bioprocesses. The established continuous-fed batch reactor system produced up to 8.2 g CMP-Neu5Ac in three consecutive productions in less than 15 h with satisfying TTNs of 91 $g_{Product}/g_{Enzyme}$. Continuous production of UDP-GlcA over 28 h resulted in a final product amount of 14.8 g and TTN of 493 $g_P/g_E$. This process enables the production of nucleotide sugars with stable product formation, requiring minimal technical equipment for multigram quantities of nucleotide sugars at the laboratory scale. Notably, the system exhibited robustness and flexibility, allowing its application to various enzymatic nucleotide sugar synthesis cascades.

## 1. Introduction

Nucleotide sugars are pivotal for many biocatalytic reactions in nature and glycan engineering. They serve as substrates for Leloir glycosyltransferases (GTs), which have been employed as reliable biocatalysts for glycan synthesis (Rexer et al., 2021). Glycans exist in every aspect of biological life and coordinate various tasks, e.g., cell-cell interactions, the effectiveness of biomolecules such as IgGs, or glycan patterns mimicked by pathogenic bacteria (Mikkola, 2020).

Nucleotide sugars have found their way to a wide application in chemistry, pharmacy, and biological research. Nucleotide sugars are used in *in vitro* glycoengineering to produce newly designed and potent antibody-drug conjugates for cancer treatment, especially in pharmacy (Wijdeven et al., 2022). *In vitro,* glycan engineering is a viable option to adjust glycan patterns to human glycoforms (Li and Wang, 2018; Wang and Lomino, 2012). Furthermore, *in vitro* glycosylation enhances the solubility of hydrophilic compounds such as flavonoids, as demonstrated by the use of Leloir-glycosyltransferases and nucleotide sugars (Khodzhaieva et al., 2021; Liu et al., 2021). A significant application of nucleotide sugars is still the high-scale production of human milk oligosaccharides (HMOs), representing a vast market with margins in the multi-kg scale every year (Walsh et al., 2020). Although most HMOs are still produced *in vivo,* the chemoenzymatic synthesis of HMOs emerges as an alternative synthesis route. New applications for HMO production have been established in the past years (Petschacher and Nidetzky, 2016). Through the extensive utilization of Leloir-glycosyltransferases, concepts for automated glycan synthesis involve nucleotide sugars as the primary substrate in enzyme reactors for the production of glycans (Hussnaetter et al., 2023). These processes demonstrate the demand for nucleotide sugars in carbohydrate research. However, nucleotide sugars lack availability and affordability since they are costly substrates (Frohnmeyer and Elling, 2023). Therefore, many processes have been established in recent years to develop a viable nucleotide sugar production pipeline.

The *de novo* synthesis and the salvage pathway of nucleotide sugars have been exploited for a proper supply process (Bülter et al., 2001; Frohnmeyer and Elling, 2023). The *de novo* synthesis uses essential monosaccharides such as glucose, mannose, or fructose, and the

* Corresponding author.
*E-mail address:* elling@biotec.rwth-aachen.de (L. Elling).

https://doi.org/10.1016/j.jbiotec.2024.09.001
Received 22 May 2024; Received in revised form 17 July 2024; Accepted 3 September 2024
Available online 4 September 2024

nucleotide sugar is enzymatically built by several steps, making enzyme cascades complex for the production of nucleotide sugars. In contrast, salvage pathways start from a monosaccharide and include two reactions. The first reaction is the phosphorylation of the anomeric C1 atom of the sugar by sugar-1-phosphate kinases and ATP. The second step comprises NDP-sugar pyrophosphorylases to convert the sugar-1-phosphate and a nucleotide (NTP) to form a nucleotide sugar (Scheme 1A) (Frohnmeyer and Elling, 2023).

Chemical or enzymatic synthesis is discussed as the most potent way for large-scale production of nucleotide sugars. However, perspectives vary, as the chemical synthesis of nucleotide sugars is generally characterized by a complex sequence of steps, low yields, and waste formation (Mikkola, 2020; Wagner et al., 2009). Enzymatic synthesis mainly contains a few enzymes, reaches high yields in a few steps, and performs in one-pot cascades. The salvage pathway enzymes in one-pot cascades are mostly applied to produce nucleotide sugars. However, processes for the large-scale production of UDP-Glc (Gutmann and Nidetzky, 2016; Orrego et al., 2017), UDP-Gal (Bülter and Elling, 2000; Fischöder et al., 2019; Mahour et al., 2022), UDP-GlcNAc (Fischöder et al., 2019), UDP-GalNAc (Bülter et al., 1997; Fischöder et al., 2019), GDP-Fuc (Fey et al., 1997; Frohnmeyer et al., 2022; Mahour et al., 2021) are challenging to scale-up. Enzymatic processes are characterized by critical parameters such as the total turnover number (TTN), which depicts the gram of product produced for each gram of enzyme used ($g_P/g_E$), which has to be extraordinarily high (Pollard and Woodley, 2007). This can limit larger-scale processes since the availability of enzymes varies with different expression organisms. Furthermore, with enzymes having a limited half-life, the process must also be assessed for the space-time yield (STY) to be most productive in a defined period and finally, the production rate (g/h) has to be assessed. This parameter is particularly valuable for comparing continuous processes to batch or repetitive-batch (rep.-batch) applications (Frohnmeyer and Elling, 2023). However, most nucleotide sugar-producing enzyme cascades still rely on batch processes conducted for 24 h or as overnight procedures, requiring a large and expensive supply of enzymes. Furthermore, batch processes are more limited by substrate inhibitions, which will

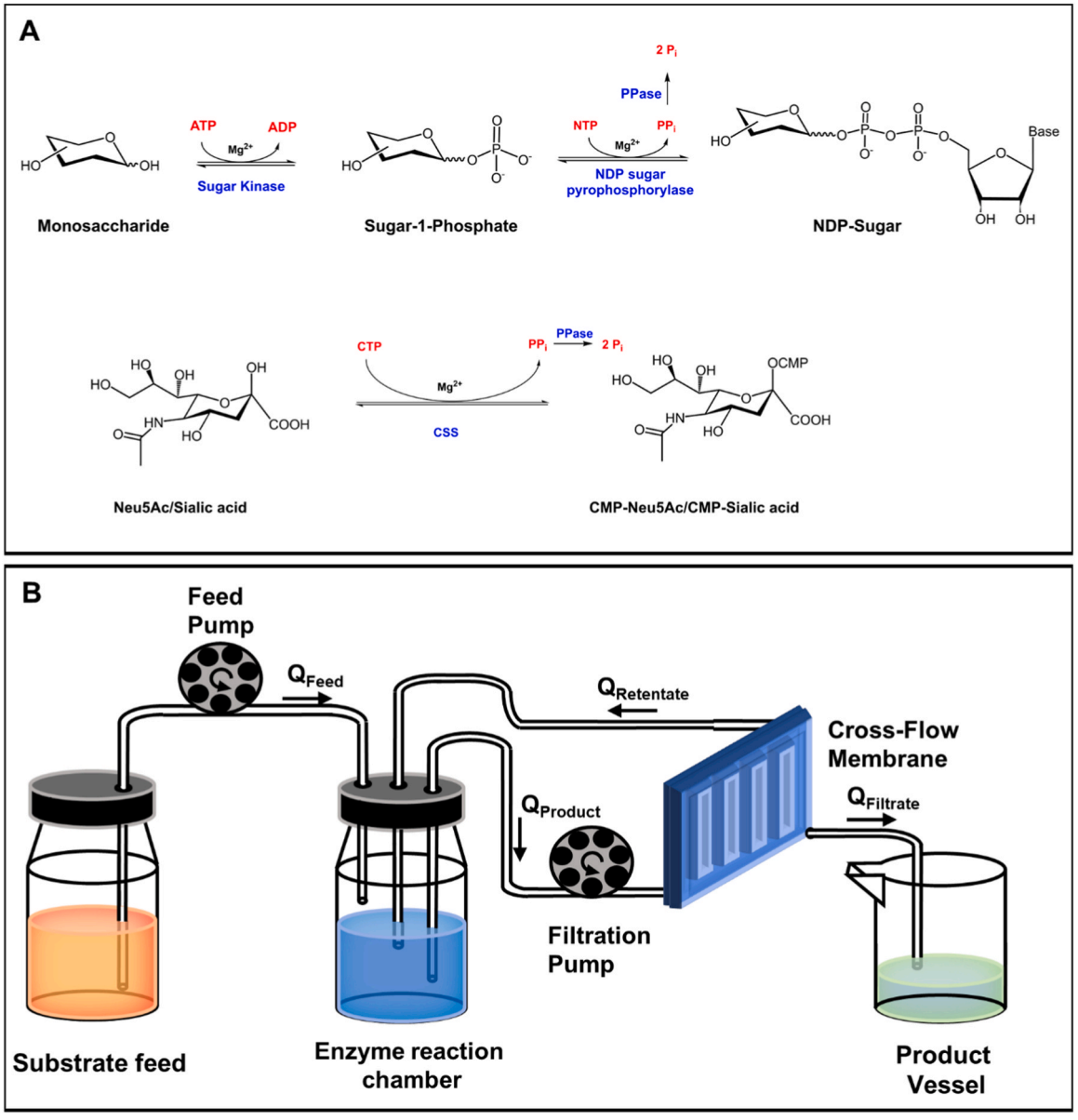


**Scheme 1.** Synthesis of nucleotide sugars with a continuous fed-batch membrane reactor. **A:** General salvage pathway for synthesizing nucleotide sugars and synthesis pathway for CMP-Neu5Ac (Frohnmeyer and Elling, 2023). **B:** General set-up of the continuous fed-batch membrane reactor for producing nucleotide sugars on a gram-scale.

significantly lengthen the process time. Some processes utilize the enzymes multiple times until the catalytic efficiency is lost. These rep.-batch processes are characterized by the separation of enzymes and products by membrane filtration. However, filtration is time-intensive and leads to prolonged production periods (Fischöder et al., 2019; Frohnmeyer et al., 2022). Some immobilization techniques, such as applying magnetic beads, were used for nucleotide sugar production (Gottschalk et al., 2021) but were not economically viable for large-scale synthesis processes.

This study presents a continuous fed-batch enzyme membrane reactor for the multi-gram production of nucleotide sugars (Scheme 1B). Featuring a simple design and cascade construction, the presented reactor is easily applied on the laboratory scale. Most importantly, the substrate solution containing the monosaccharide and nucleoside phosphate is fed into an enzyme reaction chamber. This mode provides the stepwise stack of the substrate concentration until optimal parameters for the reaction cascade are reached. This significantly reduces the substrate conversion time and avoids substrate excess inhibitions. However, substrate dilution implies that enzyme kinetics and enzyme ratios are important parameters for efficient product formation. Compared to batch syntheses, the depicted reactor system requires significantly fewer quantities of recombinant enzymes and produces comparable product volumes. Moreover, the reactor employs a membrane for continuous separation of enzymes and products, followed by recirculating the enzyme solution and remaining substrates. This strategy enhances the retention time for the enzyme reaction, promoting an improved substrate conversion. We present the multi-gram synthesis of CMP-Neu5Ac, UDP-GlcA, UDP-Gal, UDP-GalNAc, and GDP-Man in a continuous fed-batch enzyme membrane reactor. Enzyme kinetics for the cascade enzymes (Scheme S1-S5) were instrumental in optimizing enzyme ratios in one-pot batch experiments for transfer to the continuous fed-batch mode in the membrane reactor.

## 2. Materials and methods

### 2.1. Enzyme production

All enzymes used for this study were prepared according to a standardized procedure reported on multiple accounts (Eisele et al., 2018; Fischöder et al., 2019; Frohnmeyer et al., 2024; Gottschalk et al., 2022, 2021, 2019; Wahl et al., 2016, 2017).

*E. coli* strains for enzyme production (Table S1) were transformed with the respective gene-bearing plasmid by heat-shock transformation. The *E. coli* strains were then cultivated in 20 mL LB medium supplemented with 100 μg/mL ampicillin or 30 μg/mL kanamycin. Rosetta 2 (DE3) pLysS cells were supplemented with 33 μg/mL chloramphenicol. For enzyme production, 1 L Terrific Broth (TB), supplemented with the respective antibiotic, was inoculated with 20 mL overnight culture and cultivated at 37 °C. After reaching the absorbance ($OD_{600}$) of 0.6–0.8, the enzyme expression was induced with 0.1–1 mM IPTG (C. Roth, GER), the cultivation temperature was lowered to 25 °C, and the protein was expressed overnight. For the production of *Se*ManC, the medium was additionally supplemented with 10 mM $MgCl_2$. The enzymes were purified by $Ni^{2+}$-NTA immobilized metal ion chromatography (IMAC) column (HisTrap, Cytiva, SE) using an ÄKTA start (Cytiva, SE), ÄKTA purifier (Cytiva, SE) or ÄKTA Go (Cytiva, SE) system. The enzymes were dialyzed overnight in their respective storage buffer (Table S2) with a cellulose dialysis tubing (Cut-off 14 kDa; C. Roth, GER), and the protein was quantified by Bradford assay.

### 2.2. Multiplexed capillary electrophoresis (MP-CE)

As described in previous studies, MP-CE was applied and optimized to separate the nucleotides based on adenine, uridine, cytidine, and guanidine and their respective nucleotide sugars (Fischöder et al., 2019; Frohnmeyer et al., 2022; Wahl et al., 2016, 2017). MP-CE was carried out using the cePRO 9600™ system (Advanced Analytical Technologies, USA). The system consists of 96 capillaries with a total length of 80 cm, an adequate length of 50 cm, and an inner diameter of 50 μm. The separation was performed in a 50–70 mM ammonium-acetate buffer (pH 9.2) containing 1 mM EDTA (C. Roth, GER) under an electric field force of 8–12 kV. Sample injection was facilitated using a vacuum-based approach, while detection of nucleotides and the nucleotide component of the nucleotide sugar took place at 254 nm using a UV-Vis detector. Additionally, internal standards, including 1 mM of para-aminobenzoic acid (PABA; Sigma Aldrich, USA) and 4-aminophthalic acid (PAPA; Sigma Aldrich, USA), were incorporated into the analysis. All sample solutions were prepared as technical replicates, and peaks were determined according to a prepared calibration line for all nucleotides and nucleotide sugars.

### 2.3. Single capillary electrophoresis

For the product quantification, a single capillary electrophoresis was employed (Agilent 7100, Agilent, USA). This system consisted of a fused silica capillary with an effective length of 56 cm and an inner diameter of 50 μm. A 50–70 mM ammonium-acetate (C. Roth, GER) containing 1 mM EDTA (C. Roth, GER) was adjusted to a pH of 9.2. Nucleotides and nucleotide sugars were detected at 254 nm using a UV-Vis detector. To ensure accuracy, 1 mM of para-aminobenzoic acid (PABA; Sigma Aldrich, GER) was introduced as an internal standard.

### 2.4. Sugar and nucleotide kinase assays

Kinase assays were performed in a 400 μL solution containing the respective storage buffer (Table S2), supplemented with 10 mM $MgCl_2$ and 5 mM ATP. The respective substrates were added: 5 mM GlcA (*At*GlcAK), 5 mM GalNAc (*Bl*NahK), 5 mM Gal (*Ec*GalK), 5 mM Man (*Bl*NahK), 5 mM CMP (*Ec*CMPK) or 5 mM CDP (*Sc*CDPK) (Biosynth, GB). The enzymes were added to their respective substrate in varying dilutions from 1:5–1:1000. The reaction mixture was incubated at 30 or 37 °C. All synthesis reactions were stopped at 0 min, 1 min, 2 min, 3 min, 5 min, and 10 min using a stop solution (60 μL) containing 2 mM p-aminobenzoic acid (PABA), 14 mM SDS, and 2 mM 4-aminophtalic acid (PAPA) by diluting the enzyme 1:2 in the stop solution. The reaction was stopped when 10 % of the substrate was converted, and the specific activity (U/mg) was calculated accordingly. All samples were measured by MP-CE, and the peaks for ATP and ADP were quantified, which were correlated to the conversion of the sugar to the sugar-1-P.

### 2.5. N(M)DP-sugar pyrophosphorylase assays

The specific activity of NDP-sugar pyrophosphorylases was determined using the respective enzyme storage buffer (Table S2). The assay mixtures (400 μL) consisted of 10 mM $MgCl_2$ and the following substrate combinations: 5 mM UTP and 5 mM Glc-1-P for *At*USP, 5 mM UTP and 5 mM GalNAc-1-P for *Hs*AGX1, 5 mM UTP and 5 mM Gal-1-P for *Ec*GalK M173L Y311H, 5 mM GTP and 5 mM Man-1-P for *Se*ManC, and 5 mM CTP and 5 mM Neu5Ac for *Nm*CSS. In addition, each reaction contained 1 U/mL pyrophosphatase (PPase) from yeast (Sigma Aldrich, GER) to hydrolyze the emerging pyrophosphate ($PP_i$). Since GlcA-1-P is a rarely available and expensive compound, we determined the specific activity of *At*USP with Glc-1-P. Assays with *Nm*CSS contained 0.2 mM DTT in addition. Enzymes were added to their respective substrate solutions at varying dilution ratios, ranging from 1:5–1:1000, and the reactions were carried out within a controlled temperature range of either 30 or 37 °C. These synthesis reactions were stopped at designated intervals of 0, 1, 2, 3, 5, and 10 min by adding a stop solution (60 μL) containing 2 mM PABA, 14 mM SDS, and 2 mM PAPA. Each sample (60 μL) of the enzyme reaction was added to a prepared stop solution (60 μL, 2 mM PABA, 14 mM SDS, and 2 mM PAPA). The central objective of these assays was to conclude the reactions once 10 % of the substrate was converted,

allowing the subsequent specific activity calculation.

### 2.6. Kinetic assays

Kinetics for the enzymes *Hs*AGX1(Fischöder et al., 2019), *At*USP (Gottschalk et al., 2019), *At*GlcAK (Gottschalk et al., 2019), *Ec*GalK (Wahl et al., 2016), *Se*ManC (Fey et al., 1997) and *Bl*NahK for GalNAc (Nishimoto and Kitaoka, 2007) were already established. We, therefore, determined the kinetics for *Nm*CSS, *Ec*CMPK, *Sc*CDPK, and *Bl*NahK for mannose. The *Nm*CSS assays (400 µL) utilized 0.06 mg/mL *Nm*CSS with 10 mM $MgCl_2$, 2.5 mM Neu5Ac, 0.25 mM to 10 mM CTP, 0.2 mM DTT, and 100 mM HEPES pH 8. Additionally, 1 U/mL PPase (yeast) was added to the reaction, and the assays were conducted at 30 °C. The Neu5Ac kinetic assay for *Nm*CSS was done similarly, with CTP held constant at 2.5 mM while Neu5Ac varied from 0.25 mM to 10 mM. The assays for *Ec*CMPK encompassed 5 µg/mL *Ec*CMPK, 10 mM $MgCl_2$, 2.5 mM CMP, and ATP concentrations varying from 0.25 mM to 10 mM. These assays were performed in 50 mM Tris/HCl at pH 8. Similarly, assays for *Sc*CDPK were conducted with 0.6 µg/mL *Sc*CDPK, 10 mM $MgCl_2$, 2.5 mM CDP, and ATP concentrations ranging from 0.25 mM to 10 mM, also in 50 mM Tris/HCl at pH 8. For *Bl*NahK, assays were performed at 37°C. Testing *Bl*NahK with mannose, 6.3 mg/mL *Bl*NahK, 10 mM $MgCl_2$, 5 mM ATP, and mannose concentrations between 5 and 500 mM were used in a 50 mM Tris/HCl pH 8 buffer. For GTP assays, 4 mg/mL *Bl*NahK, 20 mM $MgCl_2$, 5 mM mannose, and GTP concentrations ranging from 0.125 mM to 20 mM were utilized in the same buffer.

### 2.7. Batch synthesis of nucleotide sugars

Before continuous production, the enzyme cascade reactions (Scheme S1- S6) were optimized using a batch synthesis approach. We aimed for a maximal substrate conversion within 30–60 min since the average feed and filtrate flow rate was 1.9 mL/min, corresponding to an average residence time of 31.5 min in the reactor. The detailed reaction condition of each batch experiment is described in the respective section of the supplemental information (SI).

### 2.8. General set-up of the continuous fed-batch membrane reactor

The reactor set-up consisted of a vessel containing the feed solution, a vessel serving as the reactor chamber, and a filtrate vessel (Scheme 1B). The feed and filtrate vessels were kept on ice during production, and the bottom of the reactor vessel was heated by a thermal block TH26 (HLC BioTech, GER). A Watson Marlow 101 U pump (Watson Marlow, UK) was used as a feed pump, and a Masterflex Easy Load (Sartorius, GER) was used as a filtration pump. The volumetric flow rate of the feed ($Q_{Feed}$) and the volumetric flow rate of the filtrate ($Q_{Filtrate}$) were synchronized ($Q_{Feed} = Q_{Filtrate}$). With initial flow rates of $Q_{Feed}$ and $Q_{Filtrate}$ between 2.2 mL/min and 2.5 mL/min, $Q_{Feed}$ was adjusted to compensate for the reduction of the flow rate through the membrane ($Q_{Filtrate}$) during the production. The flow of product ($Q_{Product}$) and retentate ($Q_{Retentate}$) were also synchronized with a circulation flow rate over the membrane between 150 mL/min and 250 mL/min. Polyvynilcarbon (PVC) tubing (Sartorius, GER) or commercial tubing for peristaltic pumps (PVC, Masterflex® Ismatec® pump tubing, Tygon® LMT-55, Avantor®, USA) with dimensions of 3.18 mm (inner diameter, ID), 6.35 mm (outer diameter, OD), and 1.59 mm (wall thickness) was used for the Masterflex pump. For the feed pump, a silicone tubing with the dimensions of 4.2 mm (OD), 2 mm (ID), and 1 mm (wall thickness) was used. A 100 mL borosilicate bottle served as a reactor chamber. A Vivaflow® 50 or Vivaflow® 50 R cross-flow cassette (Sartorius, GER) with a molecular weight cut-off (MWCO) of 10 kDa or 30 kDa was used for filtration. Furthermore, the membrane pressure was also controlled by a mechanical pressure indicator (Sartorius, GER).

### 2.9. Continuous production of nucleotide sugars

Exact details of the experiments for each continuous production of the nucleotide sugars CMP-Neu5Ac, UDP-GlcA, UDP-Gal, UDP-GalNAc, and GDP-Man are provided in the respective section of the supplementary information (SI).

The continuous production of nucleotide sugars was achieved by transferring the optimized reaction parameters from batch synthesis to a reactor with a volume of 50–60 mL. We aimed for a complete conversion of 10 mM substrate (comprising 10 mM monosaccharide, 10 mM ATP, and 10 mM nucleotide) to synthesize CMP-Neu5Ac, UDP-GlcA, and UDP-Gal. For UDP-GalNAc, we established a continuous production with a final product concentration of up to 20 mM. As for GDP-Man, our synthesis aimed for a maximum product concentration of 5 mM. All production processes were carried out for a minimum of 4 h to 5 h until a 500–600 mL volume had passed through the membrane. Additionally, all productions were conducted in the respective buffers: 100 mM HEPES/NaOH at pH 7.5 (UDP-GalNAc and UDP-GlcA), 100 mM HEPES/NaOH at pH 8 (UDP-Gal), or 50 mM Tris/HCl at pH 8 (CMP-Neu5Ac and GDP-Man), with the addition of 1 U/mL PPase (yeast, Sigma Aldrich, GER). The thermal block was set to either 30 °C (for CMP-Neu5Ac and GDP-Man) or 37 °C (UDP-GalNAc, UDP-GlcA, and UDP-Gal). The feed solution included 10–20 mM monosaccharide, 10–20 mM ATP, 10–20 mM UTP, and 20–30 mM $MgCl_2$ in the respective buffer.

To set up the reactor, the cross-flow membrane was initially washed with 400 mL of $ddH_2O$, and 60 mL of a prime solution containing the base buffer and $MgCl_2$ was recirculated over the membrane for 10 min while keeping the filtrate tubing closed (1st priming). In the case of CMP-Neu5Ac production, 0.2 mM DTT was added to the prime solution. After the system was primed, enzymes were added and circulated for 5 min (2nd priming). Following the 2nd priming, the filtrate tube was opened, and the feed was applied. Samples of 100 µL were collected every 60 min from the reactor vessel and the filtrate. These samples were then transferred to a stop solution containing 14 mM SDS and 2 mM PAPA and analyzed using MP-CE or single capillary electrophoresis. The product solution was stored at 4 °C until the production's end and finally at −20 °C.

### 2.10. LC-ESI-MS-analysis of nucleotide sugars from the continuous production

All solutions from the continuous productions for the nucleotide sugars CMP-Neu5Ac, UDP-GlcA, UDP-Gal, UDP-GalNAc, and GDP-Man were analyzed by a liquid chromatography-electrospray ionization mass spectrometer (Figs. S17-S25) with a Finnigan Surveyor MSQ Plus (ThermoFisher Scientific, USA), connected to a Multospher 120 RP 18 HP-3 µ column (60 mm × 2 mm; CS Chromatographie, Langerwehe, DE). A product sample of 2 mM concentration was applied to the column and eluted with 50 % (v/v) acetonitrile at a flow rate of 0.2 mL/min (needle voltage = 4 kV, temperature = 400 °C, cone voltage = 100 V, negative mode).

## 3. Results and discussion

### 3.1. General information on batch syntheses of nucleotide sugars

For all enzyme cascades (Scheme S1-S5), we first optimized the parameters for continuous production by batch synthesis experiments using the high-throughput analysis with MP-CE. The detailed results are summarized in the supplemental information and discussed in the following paragraphs. Data on enzyme concentration and conversion efficiency over time provided insight into the follow-up continuous production of the respective nucleotide sugar. The production rate (STY; $g*L^{-1}h^{-1}$) of the batch synthesis was applied since this parameter is kept constant over the production. The STY is a valuable process parameter for describing the performance of single-batch syntheses (Dias Gomes

and Woodley, 2019; Wu et al., 2021). Therefore, the determined median value of the STY is only an approximate measure of the process performance.

### 3.2. General work-flow of the continuous fed-batch membrane reactor

The reactor chamber with a constant volume of 50–60 mL contains enzymes of the respective enzyme cascade, divalent ions, and the reaction buffer. The substrate feed solution comprises 10–20 mM of monosaccharide and the respective nucleotides. The concentration of ions in both the enzyme reactor chamber and the feed solution was adjusted to be equimolar with the nucleotide concentration. Starting the fed-batch mode, substrates are diluted in the enzyme reactor chamber and mixed by the recirculation current of the filtration pump (Scheme 1B). Continuous feeding of the substrate to the enzyme reactor chamber will gradually replace the reactor volume leading to an increase in the substrate concentration in the reactor. Depending on the enzymes' $K_M$ values, the reaction velocity will increase by increasing substrate concentrations until a steady state for product formation is reached. Adjusting the flow rates of $Q_{Feed}$ and $Q_{Filtrate}$ to keep a constant reactor volume with recycling of the retentate will set the residence time of substrates and enzymes to reach a steady state conversion. In general, the development of the product concentration in the reactor provides details about the residence time, which can be estimated by dividing the time taken to reach the steady state by five. For example, feeding the 50 mL reactor with a flow rate of 2.5 mL/min for a 10 mM substrate solution leads to a substrate influx of 0.025 mmol/min. Setting the flow rate of filtrate ($Q_{Filtrate}$) and feed ($Q_{Feed}$) at 2.5 mL/min, a constant residence time of 20 min will be reached. Optimizing efficient substrate conversion within the continuous fed-batch mode is challenging, costly, and time-consuming. Therefore, the kinetic parameters of the enzymes were determined to elucidate limitations. Enzyme concentrations were optimized to reach full substrate conversion in the range of the residence time of the reactor. Overall, the established continuous fed-batch reactor system leads to the synthesis of multigram quantities of nucleotide sugars in a single working day while utilizing relatively small quantities of biocatalyst.

### 3.3. Production of CMP-Neu5Ac

We applied an enzyme cascade employing *Ec*CMPK, *Sc*CDPK, and *Nm*CSS to start the synthesis of CMP-Neu5Ac from CMP and Neu5Ac (Scheme S1). The system was chosen since CMP is up to ten times cheaper than CTP. ATP is utilized to form CDP (*Ec*CMPK) and CTP (*Sc*CDPK) and is subsequently used for the CMP-Neu5Ac formation (*Nm*CSS). ATP is a necessary component for this process and falls within the price range of 0.50 € to 0.80 € per gram and has only a minor impact on the production costs. Furthermore, we aimed to demonstrate the repetitive use of the enzymes without changing the cross-flow membrane (Fig. 1).

Kinetic measurements of the enzymes revealed high specific activities of 76.8 U/mg (*Nm*CSS), 225 U/mg (*Ec*CMPK) and 1700 U/mg (*Sc*CDPK) (Table S3). The activities of all enzymes in the reactor were adjusted to 20 U/mL while the enzyme concentration was utilized based on the specific activities, previously determined in the enzymatic activity assays. The optimized batch cascade with 20 U/mL of each enzyme resulted in 8.75 mM (97 % yield for 10 mM substrate concentration) CMP-Neu5Ac in less than 30 min (Fig. S2 and Table S4). For the transfer to the continuous fed-batch reactor, the low $K_M$ values of all enzymes suggest that substrate dilution will not limit substrate conversion. The flow rates of filtrate ($Q_{Filtrate}$) and feed ($Q_{Feed}$) were adjusted to reach a residence time of 31.5 min for effective conversion of the substrates (Fig. 1). For this particular production, we tested the consecutive usage of the enzyme cascade by intermediate overnight storage at 4 °C as well as the performance of the cross-flow membrane. Therefore, the production was carried out for three consecutive days with a production time of 4.5 h (d1), 4 h (d2), and 4.8 h (d3). On d1, the reactor reached full saturation of 10.7 mM CMP-Neu5Ac after 2 h which decreased to a constant level at 8.9 mM. The production of d2 started with a concentration of 10 mM CMP-Neu5Ac, as residual substrates in the reactor vessel were fully converted during overnight storage. On d2, the product concentration decreased from 10 mM to 6 mM during the first 30 min (Fig. 11, d2, 4.5 h). The steady state was reached at 8.2 mM after 6 h and increased to 8.7 mM. On d3, the reactor started with an initial product concentration of 10 mM which dropped to 8.0 mM at the 9 h mark

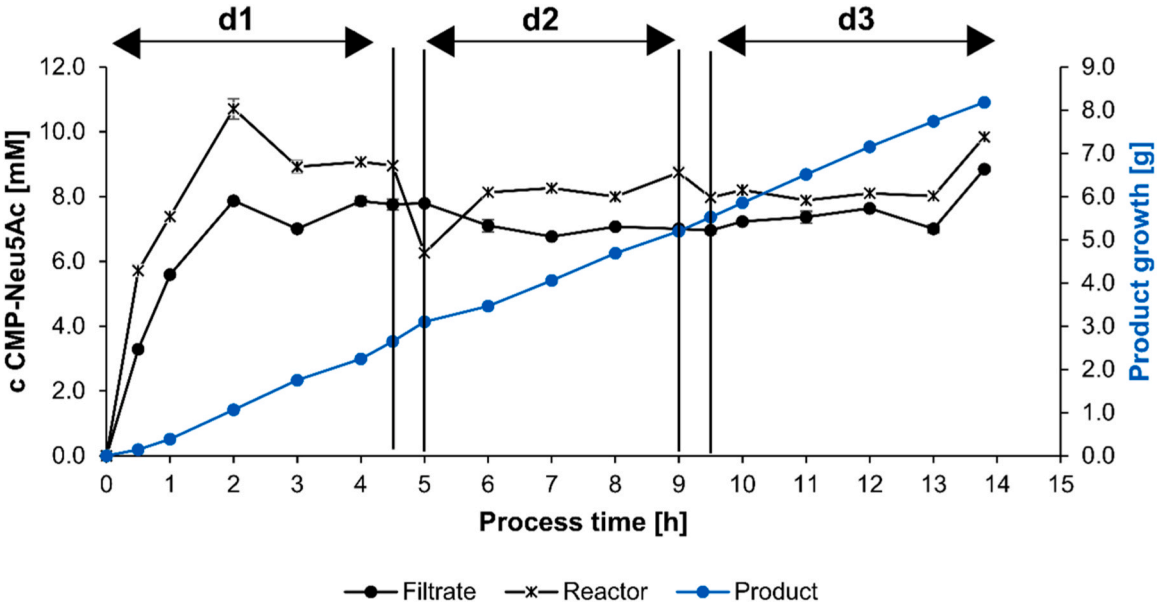


**Fig. 1.** Continuous production of CMP-Neu5Ac starting from CMP and Neu5Ac. The production was performed over three consecutive days, and the enzyme solution (reactor vessel) was stored overnight at 4 °C. The feed contained 10 mM Neu5Ac, 10 mM CMP, 20 mM ATP, 0.2 mM DTT, 30 mM $MgCl_2$, and 100 mM HEPES pH 7.5. The reactor vessel featured a 60 mL volume with 20 U/mL *Ec*CMPK, 20 U/mL *Sc*CDPK, 20 U/mL *Nm*CSS, and 1 U/mL PPase (yeast). The continuous flow from the feed ($Q_{Feed}$) to the reactor was balanced to match the filtrate flow ($Q_{Filtrate}$) within the range of 2.3 mL/min to 3.1 mL/min ($Q_{Feed} = Q_{Filtrate}$). A PES cross-flow membrane with a 10 kDa MWCO was utilized. The recirculation rate of the retentate ($Q_R$) and the product solution to the membrane ($Q_P$) was set to a flow rate between 130 mL/min and 140 mL/min. T=30 °C.

(Fig. 11, d3, 9 h). The CMP-Neu5Ac concentration reached a constant level and a notable increase to 9.8 mM at 14 h as seen on d2 at 9 h. We believe that this is directly connected to the decreasing flow rate of feed ($Q_{Feed}$) and filtrate ($Q_{Filtrate}$).

The flow rates for the two productions started at 3.1 mL/min (d2) and 2.5 mL/min (d3). Only the flow rate of the production on d1 increased after 4.5 h but did not affect the production (Fig. S3A-C). However, the flow rates on d2 and d3 dropped at the end of the production, leading to a slight increase in production efficiency. We assume that the drop in the flow rate brought the cascade within the kinetic linear range of the enzymes.

In summary, after three days of production, we gained a pool of all filtrates containing a product concentration of 7.1 mM, translated to a final product amount of 8.2 g (Table S5). The enzyme cascade with *Ec*CMPK, *Sc*CDPK, *Nm*CSS, and PPase (yeast) achieved a substantial STY of 4.6 $g*L^{-1}h^{-1}$, laying within a significant range for fine chemicals. This enzyme cascade demonstrates that the reactor system is capable of working with cascades of at least four different enzymes. Furthermore, the fed-batch membrane reactor can be utilized over several hours in a continuous mode and is also flexible enough to continue production the next day with the employed enzyme cascade.

### 3.4. Production of UDP-GlcA

The enzyme cascade for the synthesis of UDP-GlcA was previously described in our group in the context of hyaluronic acid synthesis (Gottschalk et al., 2021, 2019). We adopted the enzyme cascade, including *At*GlcAK, *At*USP, and PPase (yeast), for the gram-scale production of UDP-GlcA (Scheme S2). Kinetic parameters were deducted from our previous study (Gottschalk et al., 2019) (Table S3) to further optimize the synthesis cascade in batch experiments. A critical point for optimization is the substrate inhibition by ATP ($K_{iS}$= 2.87 mM) (Gottschalk et al., 2019). With an apparent $K_M$ of 8.56 mM (ATP) and a $K_M$ of 0.62 mM for GlcA, *At*GlcAK shows a relatively low activity compared to *At*USP. In addition, *At*USP is a promiscuous enzyme accepting GlcA-1-P among other sugar phosphates. However, since GlcA-1-P is barely available, kinetics in our previous study were performed with Glc-1-P (Gottschalk et al., 2021) (Table S3) and served to approximate optimal conditions in the enzyme cascade. These kinetic features demanded careful adjustment of the enzyme cascade and reaction conditions. The batch experiment data revealed that 0.3 U/mL *At*GlcAK and 21 U/mL *At*USP are sufficient to synthesize up to 10 mM UDP-GlcA (91 % yield) in 60 min (Fig. S4).

A first continuous fed-batch synthesis reached complete substrate conversion after 4 h, which continued up to 6 h with a final yield of 88 % and stable STY of 5.1 $g*L^{-1}h^{-1}$ (Fig. S5 and Table S5). We concluded that the enzyme cascade is stable enough to perform a long-term synthesis over 28 h (Fig. 2). The reactor system synthesized up to 14.8 g of UDP-GlcA (76 % yield) over 28 h, while keeping the product concentration stable at values between 9 mM and 10 mM for the first 22 h. However, beyond 22 h, the product concentration decreased indicating process destabilization most likely because of enzyme degeneration. A further aspect of the process was the continuous reduction of the filtrate flow rate, which was counteracted by increasing the flow rate of the membrane pump up to 300 mL/min at the 24 h mark (Fig. S6). We assume that this led to further destabilization as the enzymes were subjected to increasing share forces. The process yielded an excellent TTN and productivity of 493 $g_P/g_E$ and 0.54 g/h, respectively (Table S5), displaying even comparable results to the production of CMP-Neu5Ac.

Maintaining a constant flow rate throughout the entire process was challenging due to membrane fouling, which led to a decrease in the flow rate of $Q_{Filtrate}$ (Fig. S6). Increasing the flow rate of the membrane pump could not compensate for the reduction of $Q_{Filtrate}$. In addition, the membrane with 30 kDa MWCO was less suitable for the intended production mode. We assume that *At*GlcAK could have clogged the membrane when the TMP was not maintained, as it has a MW of 47.5 kDa. The long-term production of UDP-GlcA could potentially exhibit improved performance with a 10 kDa PES membrane, as it worked better for the process as demonstrated for the production of CMP-Neu5Ac.

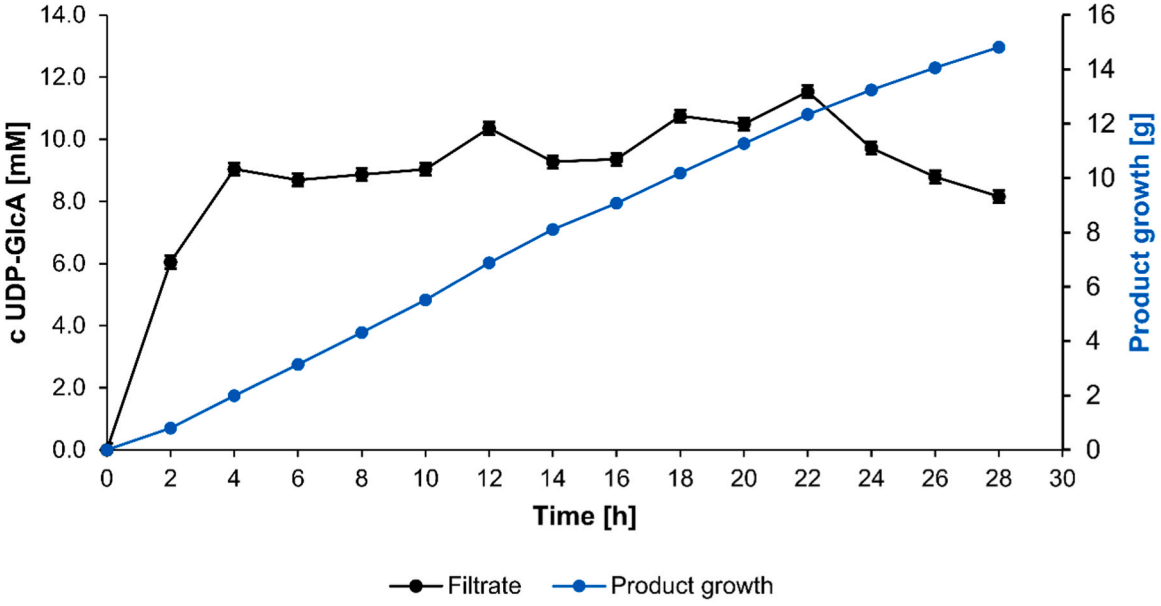


**Fig. 2.** Continuous production of UDP-GlcA in the continuous fed-batch membrane reactor. The reactor (reaction volume 60 mL) was fed with a feed solution comprising 12 mM ATP, 12 mM UTP, 12 mM GlcA, 25 mM $MgCl_2$, and 100 mM HEPES pH 8 at 37°C. The reactor vessel contained 0.3 U/mL *At*GlcAK, 21 U/mL *At*USP, and 1 U/mL PPase (yeast). A cellulose membrane with a 30 kDa MWCO was used as a cross-flow cassette. The feed ($Q_{Feed}$) and filtrate flow ($Q_{Filtrate}$) were synchronized at an average of 1.9 mL/min. The flow rate over the membrane ($Q_{Prodcut}$) and retentate was adjusted to retain the flow rate of $Q_{Filtrate}$ and $Q_{Feed}$ and was adjusted between 130 mL/min and 300 mL/min. T= 37 °C.

### 3.5. Production of UDP-Gal

The salvage pathway describes the enzymatic synthesis of UDP-Gal, based on a galactokinase (GalK) and a UDP-sugar pyrophosphorylase (USP) (Frohnmeyer and Elling, 2023). Enzymes from several strains were used for the gram scale production of UDP-Gal including GalK from *Streptococcus pneumoniae* (Zou et al., 2013) or *Escherichia coli* (Wahl et al., 2016) and USP from either *Hordeum vulgare*(Wahl et al., 2017) or *Arabidopsis thaliana* (Li et al., 2021). However, it was shown that the *Ec*GalK wild type was less stable than the mutant variant M173L/Y371H, and the mutant was used for several syntheses of UDP-Gal (Fischöder et al., 2019; Wahl et al., 2016). For gram scale synthesis, we used the *Ec*GalK M173L/Y371H variant and *At*USP (Scheme S3) since this pyrophosphorylase was demonstrated to be very stable for the continuous production of UDP-GlcA. The kinetics of *Ec*GalK M173L/Y371H revealed a significantly lower activity than *At*USP (Table S3). Therefore, the *Ec*GalK M173L/Y371H activity was adjusted to reach full conversion of 10 mM Gal, ATP, and UTP in 30 min in batch synthesis (Fig. S7).

The process was performed for 6.5 h, reaching the steady-state after 2 h at 10 mM (Fig. 3). The continuous production yielded a final concentration of 8.4 mM and product quantity of 2.5 g UDP-Gal achieving a productivity of 0.39 g/h with a TTN of 28 $g_P/g_E$ (Table S7). Overall, the production of UDP-Gal in continuous mode is feasible. Other galactokinases for more effective product conversion may improve productivity.

### 3.6. Production of UDP-GalNAc

UDP-GalNAc is one of the most precious main nucleotide sugars and, most interesting for establishing a production process (Frohnmeyer and Elling, 2023). Over the past years, some processes have been designed to produce UDP-GalNAc in the higher gram scale (Fischöder et al., 2019; Li et al., 2021; Zhao et al., 2010). The most dominant synthetic route is based on the salvage pathway enzymes *N*-acetyl-hexokinase (NahK), either from *Bifidobacterium longum* (Fischöder et al., 2019) or *Bifidobacterium infantis* (Li et al., 2021; Zhao et al., 2010) and the human enzyme UDP-*N*-acetylgalactosamine diphosphorylase (AGX1) (Bourgeaux et al., 2005; Fischöder et al., 2019). We used the combination of *Bl*NahK and *Hs*AGX1 (Scheme S4) in the continuous production system since this enzyme cascade is well described and readily applicable for UDP-GalNAc and UDP-GlcNAc synthesis (Fischöder et al., 2019; Frohnmeyer and Elling, 2023).

We aimed for a maximal substrate conversion in a 30 min reaction and kept this as residence time in the continuous reactor. In our previous study, an enzyme ratio of 2 U/mL *Bl*NahK and 2 U/mL *Hs*AGX1 worked well with high conversions in 30 min in repetitive-batch mode (Fischöder et al., 2019). To further speed up the conversion in the direction of the nucleotide sugar, an excess of *Hs*AGX1 was applied (Frohnmeyer et al., 2024). The most effective product formation was gained using 6 U/mL *Bl*NahK and 24 U/mL *Hs*AGX1 in a batch experiment (Fig. S9). Upscaling these enzyme ratios, however, would mean that up to 375 mg *Bl*NahK and 120 mg *Hs*AGX1 are required for a 50 mL reactor volume which contradicts the rationale for developing an economically viable enzyme cascade. We considered increasing the substrate concentration to justify the high enzyme concentrations as this would enhance the STY and TTN. However, orthophosphate is formed by enzymatic cleavage of $PP_i$ (Scheme 1A). Moreover, magnesium-phosphate precipitation occurs at higher substrate concentrations, reducing the efficiency of the reactor (Kragl et al., 1996). To define an upper limit for the substrate concentration at which no magnesium-phosphate precipitates are formed, amounts of orthophosphate expected from a full conversion of a nucleotide sugar synthesis cascade were mixed with the respective $Mg^{2+}$ amounts used for full nucleotide saturation in the production buffer (Fig. S10). We observed precipitation of magnesium-phosphate starting at 60 mM $P_i$ and 60 mM $Mg^{2+}$ which translates to a synthesis with complete conversion (>99 %) of 30 mM ATP, UTP, and GalNAc. Increasing the $P_i$ and $Mg^{2+}$ concentrations further intensified the magnesium-phosphate precipitation. We concluded that the reactor performance is limited to substrate concentrations of 20 mM to 30 mM and a *Bl*NahK/*Hs*AGX1 ratio of 1:5 favors product yield, process development, and a high TTN.

A first continuous fed-batch production was performed (Fig. S11) with 11 mM substrate concentration (Fig. S11). The reactor showed stable productivity and constant flow rates over 9 h (Fig. S12A). The production gained 4.6 g UDP-GalNAc with a yield of 85 % with a notable productivity rate of 0.51 g/h with an average STY of 5.2 $g*L^{-1}h^{-1}$ and TTN of 52 $g_P/g_E$ (Table S8). To enhance the TTN further, the substrate concentrations were increased to 21 mM (Fig. 4, d1). The initial flow rate of 3 mL/min (Fig. S12B) reduced the residence

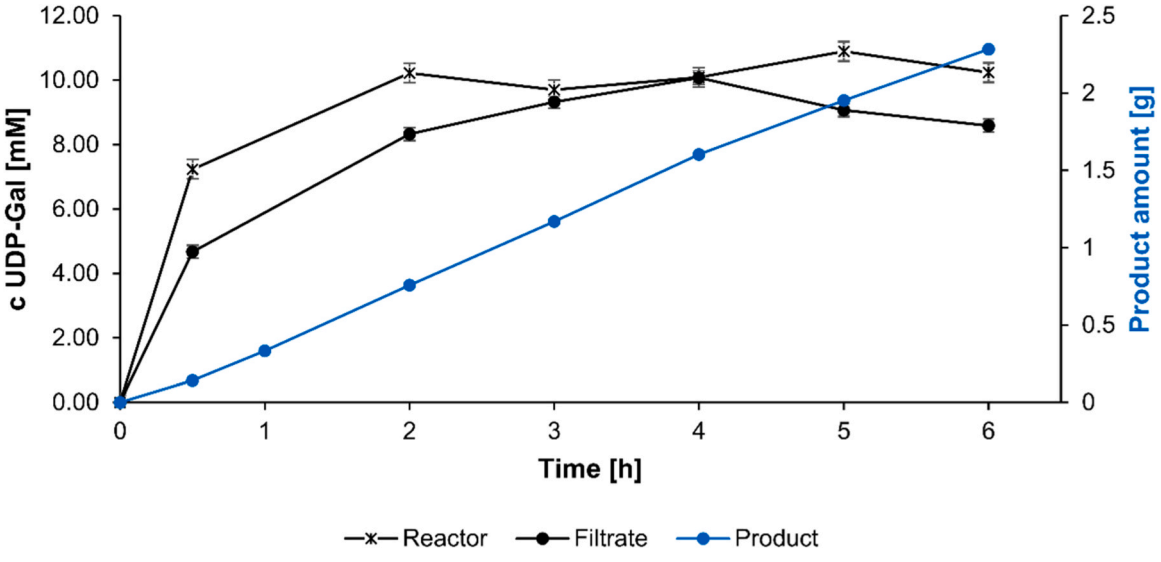


**Fig. 3.** Continuous production of UDP-Gal in the continuous fed-batch membrane reactor. The feed contained 10 mM ATP, 10 mM UTP, 20 mM $MgCl_2$, 10 mM Gal, and 100 mM HEPES pH 8. 700 mU/mL *Ec*GalK M173L/Y371H, 16 U/mL *At*GlcAK and 1 U/mL PPase (yeast) were used in the reactor chamber. The flow rate between feed ($Q_{Feed}$) and Filtrate ($Q_{Filtrate}$) was adjusted at 2.5 mL/min by setting the recirculation rate over the membrane between 100 mL/min and 180 mL/min. A PES cross-flow membrane with an MWCO of 10 kDa was used. T=37 °C.

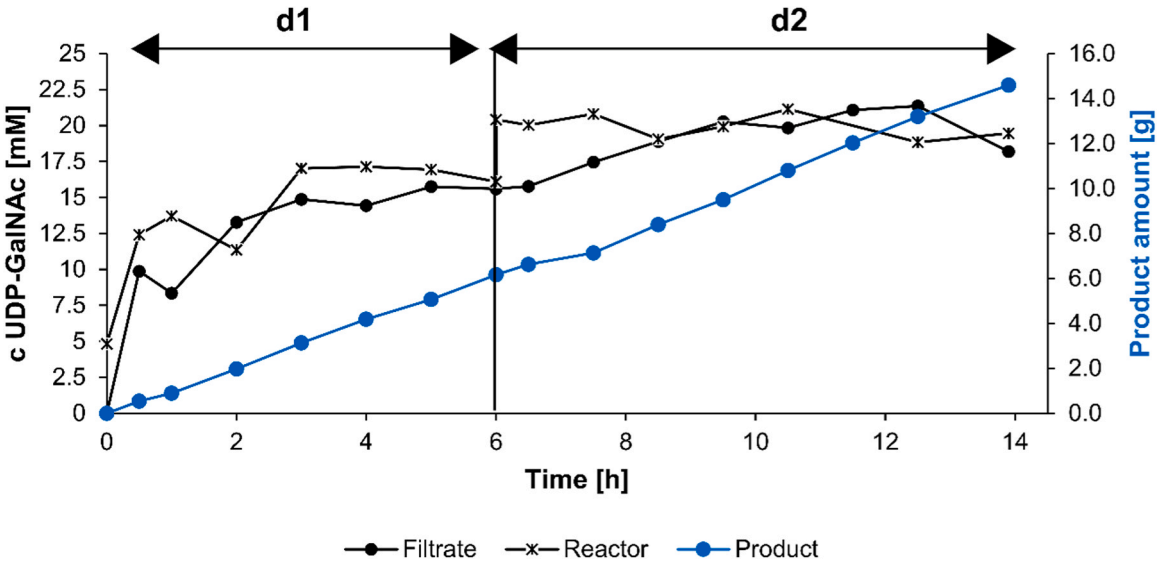


**Fig. 4.** Elongated run of the continuous reactor for the synthesis of UDP-GalNAc. **d1:** The feed solution contained 21 mM ATP, 21 mM UTP, 22 mM $MgCl_2$, 21 mM GalNAc, and 100 mM HEPES pH 8. 2 U/mL *Bl*NahK, 10 U/mL *Hs*AGX1 and 1 U/mL PPase (yeast) were used in the reactor chamber. **d2:** The feed solution was prepared with 21 mM ATP, 21 mM UTP, 22 mM $MgCl_2$, 21 mM GalNAc, and 100 mM HEPES pH 8. The reactor chamber was supplemented with 50 U *Bl*NahK and 250 U *Hs*AGX1, and the chamber volume was reduced to 50 mL, resulting in a final enzyme concentration of 2 U/mL *Bl*NahK and 10 U/mL *Hs*AGX1. The flow rate for both production days was set between feed ($Q_{Feed}$) and filtrate ($Q_{Filtrate}$) at 1.6 mL/min by setting the recirculation rate over the membrane between 120 mL/min and 140 mL/min. A PES cross-flow membrane with an MWCO of 10 kDa was used. T= 37 °C.

time to 17 min leading to a decreased substrate conversion (Fig. 4, d1). The adjustment of the flow rate to reach a $Q_{Filtrate}$ of approximately 2.3 mL/min elongated the residence time to approximately 22 min and enabled the synthesis to continue over a longer duration. Despite the high initial flow rate, a steady state was reached between 3 h and 6 h with product concentrations between 14.8 mM (3 h) and 15.8 mM (6 h) (Fig. 4, d1). The production performed exceptionally well, producing a final product amount of 6.2 g UDP-GalNAc in 6 h (13.5 mM, 68 % yield) (Table S8). Although substrates were not fully converted, the reactor still reached a high productivity of 1.1 g/h and an excellent average STY of 8.4 $g*L^{-1}h^{-1}$ with a TTN of 93 $g_P/g_E$.

To continue with the production, the enzyme-containing reactor vessel from d1 was stored overnight at 4°C for subsequent use (Fig. 4, d2). On d2, the reactor was supplemented with 50 U *Bl*NahK and 250 U *Hs*AGX1, to an overall biocatalytic load of 163 mg (for details see supplementary information). Additionally, overnight storage ensured that the remaining substrate from the first production (d1) was converted entirely, resulting in an initial product concentration of 20.4 mM on d2. The concentration of UDP-GalNAc remained between 18.8 mM and 21 mM for 7.4 h during the production on d2. Furthermore, a lower flow rate of 1.6 mL/min was used and was stable over the production period with only minor fluctuations between 2 h and 3 h (Fig. S12C). With the elongation of the production time and a higher biocatalyst load, 8.4 g of UDP-GalNAc (Table S8) was synthesized. Compared to the production on d1, the STY effectively doubled to 11.5 $g*L^{-1}h^{-1}$. Moreover, a productivity of 1.14 g/h demonstrates a significant enhancement of the reactor set-up.

### 3.7. Production of GDP-Man

Enzyme cascades for the synthesis of GDP-Man are well established. The most common cascade is deducted from the *de novo* pathway, which starts with the formation of Man-6-P by hexokinase and is followed by isomerization to Man-1-P by a phosphomannomutase (ManB) and the nucleotide sugar synthesis by a GDP-Mannose pyrophosphorylase (ManC) (Elling et al., 1996; Frohnmeyer and Elling, 2023; Mahour et al., 2021; Rexer et al., 2018). An alternative route exploits the promiscuity of *Bl*NahK to phosphorylate Man at the C1 position using ATP or GTP and the pyrophosphorylase ManC from *Pyrococcus furiosus* (Li et al., 2013, 2021; Wang et al., 2022). We used the *Bl*NahK and a GDP-Mannose pyrophosphorylase from *Salmonella entericia* (*Se*ManC), which was also utilized for continuous production in a previous study (Fey et al., 1997) and established a cascade that used ATP as the primary phosphate donor and GTP for the sugar activation (Scheme S5). Kinetic experiments revealed a low affinity of *Bl*NahK for mannose (Table S3) and, therefore, the necessity for high mannose concentrations in batch experiments. The activity of *Bl*NahK is significantly enhanced by the high excess of Man (Fig. S13), which was also beneficial for the one-pot batch synthesis of GDP-Man (Fig. S14).

Continuous production with 50 mM Man and 10 mM ATP in the substrate feed solution resulted in a low yield of 45 %, an inefficient TTN of 4 $g_P/g_E$, and a low productivity of 0.13 g/h (Fig. S15 and Table S9). Given the inefficiency, a new approach for the GDP-Man production was implemented (Fig. 5). The reactor chamber was set up to contain 50 mM Man 10 mM $MgCl_2$, and enzymes. The substrate feed solution contained 50 mM Man, 5 mM ATP, 6 mM GTP, and 10 mM $MgCl_2$.

With this experimental design high excess of Man to ATP was maintained in the reaction chamber, promoting the *Bl*NahK reaction and supporting the reaction in the GDP-Man synthesis direction. Most importantly, full conversion of the substrates ATP and GTP was observed in the reaction chamber, an outcome not reflected in the filtrate. Here, the steady state was reached at concentrations of 3.3 mM, which reached a final concentration of 3.8 mM after 6 h (Fig. 5). Fluctuations in the flow rate ($Q_{Filtrate}$) are noticeable, however, without a significant impact on the enzyme cascade reactions. A total biocatalyst load of 160 mg resulted in a final yield of 63 % and a TTN of 8.8 $g_P/g_E$. The final amount of 1.4 g GDP-Man is translated to a productivity of 0.22 g/h and STY of 2.4 $g*L^{-1}h^{-1}$ (Table 1) exceeding the first production (Fig. S15, Table S9). In summary, the continuous fed-batch membrane reactor allows the application of an enzyme cascade with an unnatural substrate in high concentration. However, the economic feasibility depends on the product, and GDP-Mannose may not be economically compelling enough for this production mode. Further optimization of *Bl*NahK, particularly regarding $K_M$ values and specific activity towards Man, is demanding to enhance the gram-scale production of GDP-Man. The presented GDP-Man synthesis expands the product range of the reactor

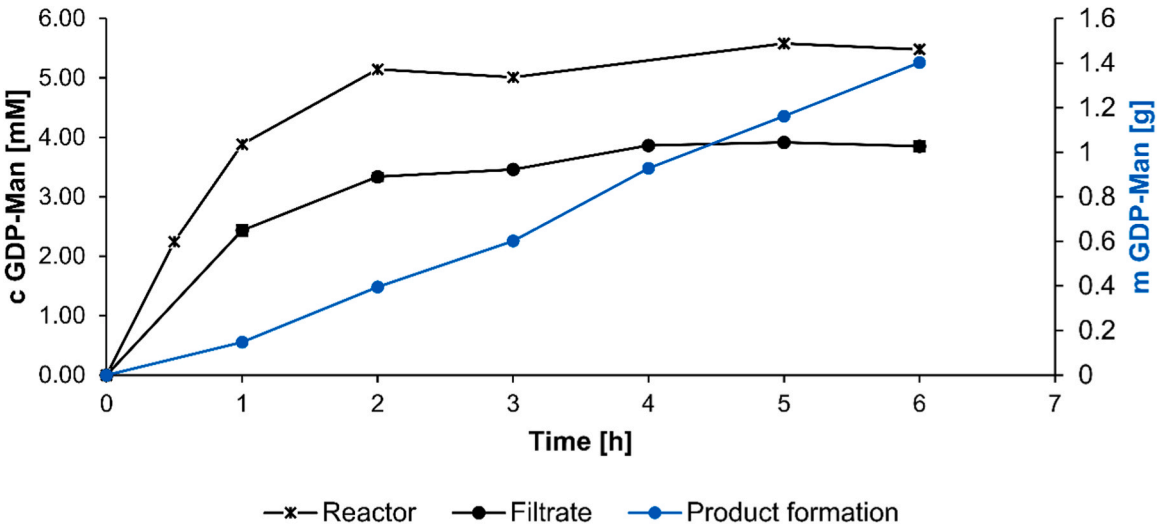


**Fig. 5.** Continuous production of GDP-Man with high Mannose excess. The reactor chamber contained 50 mM Man, 2.5 mg/mL *Bl*NahK (0.7 $U_{Man}$/mL), 1.5 U/mL (0.5 mg/mL) *Se*ManC, 1 U/mL PPase (yeast), and 10 mM $MgCl_2$. The feed solution contained 5 mM ATP, 6 mM GTP, 50 mM Man, 10 mM $MgCl_2$, and 50 mM Tris/HCl pH 8. The filtrate (QFiltrate) flow rate was adjusted to the feed (QFeed) flow rate, corresponding to values between 2.5 mL/min to 1.6 mL/min. T=37 °C.

**Table 1**
Nucleotide sugar production in the continuous fed-batch membrane reactor.

| Nucleotide sugar | Yield [%] | STY[a] [g*L$^{-1}$h$^{-1}$] | Product [g] | TTN [$g_P$/$g_E$] | Productivity [g/h] |
|---|---|---|---|---|---|
| CMP-Neu5Ac (CMP) | 80 | 4.6 | 8.2 | 91 | 0.57 |
| UDP-GlcA | 76 | 5.3 | 14.8 | 493 | 0.54 |
| UDP-Gal | 84 | 4.9 | 2.5 | 28 | 0.39 |
| UDP-GalNAc[b] | 68<br>88 | 8.4<br>11.5 | 6.2<br>8.4 | 93<br>72 | 1.08<br>1.14 |
| GDP-Man | 63 | 2.4 | 1.4 | 9 | 0.22 |

[a] : Values depict the median value.
[b] : the production parameters for d1 and d2 (Fig. 4, Table S8).

system and demonstrates its flexibility.

### 3.8. Comparison of the continuous fed-batch membrane reactor with other enzymatic production processes

The continuous fed-batch membrane reactor demonstrates high performance for nucleotide sugar production (Table 1). Previous studies report batch and continuous processes displaying distinct productivities, STYs, and TTNs (Frohnmeyer and Elling, 2023).

In this study, the production of CMP-Neu5Ac from CMP was very robust over three consecutive days with a final product amount of 8.2 g after 14 h with a reasonable TTN of 91 $g_P/g_E$ and a productivity of 0.57 g/h. A previous study demonstrated the continuous synthesis of CMP-Neu5Ac in an enzyme membrane reactor by feeding the substrate CTP over 40 h. This approach reached multi-gram amounts of the nucleotide sugar with an STY of 10.6 g $L^{-1}$ $h^{-1}$ and an overall conversion of 78 % (Kragl et al., 1996).

The continuous synthesis of UDP-GlcA yielded the highest product amount (14.8 g) with the best TTN (493 $g_p/g_E$) (Table 1). A production protocol for UDP-GlcA was reported, employing UDP-Glc dehydrogenase starting from UDP-Glc and an $NAD^+$ cofactor regeneration system. In a single-batch reaction, 2.76 g of UDP-GlcA was produced (87 % yield) on a 500 mL scale (Wang et al., 2022). The batch production resulted in an average productivity of 0.23 g/h for an overnight incubation. In the continuous fed-batch process, it is possible to produce UDP-GlcA with a productivity of 0.54 g/h to 0.6 g/h (Table 1). In contrast, the single-batch reaction had to be scaled threefold to remain competitive and would entail a significant increase in the demand for biocatalyst and UDP-Glc (Wang et al., 2022).

For UDP-GalNAc, we achieved productivity of over 1 $g_{Product}$/h, underscoring the high performance of the reactor system (Table 1). The continuous production was scaled up to higher initial substrate concentrations (20 mM), however, being limited by precipitation of magnesium-phosphate. Most interestingly, two consecutive runs of the reactor demonstrate the robustness of the reactor and membrane module. In comparison to the established repetitive (rep.)-batch synthesis of UDP-GalNAc (Fischöder et al., 2019), lower STYs and TTNs are reached. However, these values are not easily comparable since substrate concentrations of 20 mM were not applied in the rep.-batch production. The rep.-batch mode mainly depends on the proportionality of time and conversion efficiency. Increasing the substrate concentration at a constant catalytic load will prolong the synthesis time to a full conversion. Additionally, the process time for the repetitive filtration steps has to be considered leading to a decrease in productivity.

UDP-Gal production in the continuous fed-batch membrane reactor falls firmly behind the rep.-batch synthesis (TTN of 494 $g_P/g_E$., 0.64 g/h productivity) (Fischöder et al., 2019). However, including a processing time of 30 min for each centrifugation step the overall production time reaches 60 min for each batch and drops productivity to 0.32 g/h. With this parameter included, continuous production becomes comparable to the rep.-batch. Another study reports the UDP-Gal synthesis with crude extracts which contained up to five enzymes and an ATP regeneration system with polyphosphate. In a 1 L-batch reactor 23.4 g of UDP-Gal were produced in 24 h with a TTN of 20 $g_P/g_E$ (Mahour et al., 2022). In comparison, the TTN of the continuous reactor system turns out to be slightly more effective.

The synthesis of GDP-Man proved to be the most challenging. The continuous reactor system was adjustable for the conversion of an unnatural substrate and reached reasonable productivity Table 1. In comparison, it is still better, when compared to a continuous production in an EMR on a gram scale reaching an STY of 1.17 g*$L^{-1}h^{-1}$ (Fey et al., 1997).

The cascade for producing CMP-Neu5Ac included cost-effective *in-situ* synthesis of CTP from CMP, but we opted against in-situ UTP production from UMP. Although *Ec*CMPK and *Sc*CDPK can theoretically produce UTP with ATP, their efficiency is lower (Jeudy et al., 2006, 2009). Implementing an ATP regeneration system using PPKs and polyphosphate is another option (Mahour et al., 2022, 2021), but high polyphosphate concentrations cause membrane blockage and hamper

nucleotide sugar purification (Kulmer et al., 2017). *In-situ* ATP synthesis was not considered due to its low cost, but removing inhibitors like ADP could improve synthesis efficiency (Frohnmeyer et al., 2022, 2024).

In summary, the continuous fed-batch reactor showcased a versatile applicability to most of the previously described enzyme cascades. The relatively simple setup of the reactor system enabled us to produce gram amounts of nucleotide sugars on the lab scale. We see great potential for enhanced nucleotide sugar production with further refinement of the reactor system.

### 3.9. Purification of nucleotide sugars

Enzymatic nucleotide sugar productions are primarily conducted in diluted solutions where the product is accumulated in substantial volumes. However, the product separation from highly diluted solutions is a great concern. Especially in the case of nucleotide sugars, since the purification by chromatography can be labor- and energy-intensive. Furthermore, a nucleotide sugar solution has to be separated from spent nucleotides deriving from the anomeric phosphorylation step. Additionally, some nucleotide sugars are unstable in diluted mixtures and the presence of metal ions. However, efficient strategies for nucleotide sugar purification have been developed in recent years (Frohnmeyer and Elling, 2023).

The most classical way for nucleotide sugar purification was already described 20 years ago for the purification of CMP-Neu5Ac, which included the combination of anion exchange (AEC) and size exclusion chromatography (SEC), directly followed by lyophilization (Kragl et al., 1996; Lemmerer et al., 2016; Song et al., 2003). However, with multi-gram amounts of nucleotide sugars, protocols have to be adapted. The purification of UDP-Glc included the precipitation of the nucleotide sugar by adding EtOH and monovalent ions to the fraction from AEC separation (Lemmerer et al., 2016). Product purities between 81 % and 95 % were reached (Lemmerer et al., 2016). We used an extended purification protocol to purify GDP-Fuc, including dephosphorylation of nucleoside mono-, di- and triphosphates by adding alkaline phosphatase (AP) to an enzyme-free product solution. After the removal of AP by ultrafiltration, the nucleotide sugar solution was supplemented with $Mg^{2+}$ and >95 % of orthophosphate, and was then precipitated by adding 2-propanol. Increasing the 2-propanol in the supernatant finally precipitated GDP-Fuc with a product recovery of 77 % (Frohnmeyer et al., 2022). For UDP-6-azido-GalNAc, we reached an HPLC purity of 99.5 % by AP treatment and AEC (Frohnmeyer et al., 2024). Further fine purification by medium-pressure liquid chromatography (MPLC), cation exchange chromatography, and evaporation gave 2.1 g UDP-6-azdio-GalNAc (81 % recovery) with a final HPLC purity of 99.96 % (Frohnmeyer et al., 2024). Further purification methods included the purification of GDP-Gal by establishing a precipitation protocol of GDP-Gal, which conclusively gained a recovery of 92.0 % and a purity of 99.9 % (Ohashi et al., 2017). AEC purification procedures were applied to product solutions containing GDP-Fuc or UDP-Gal and polyphosphate giving product purities of >90 % HPLC purity (Mahour et al., 2022, 2021). For the nucleotide sugar solutions of this study, purification protocols, including AP treatment, precipitation, and chromatographic steps, were established by our industrial partner as previously described (Frohnmeyer et al., 2024).

## 4. Conclusion

We established an effective laboratory process for producing nucleotide sugars on a multi-gram scale in a continuous fed-batch membrane reactor. The robustness of the continuous process allows maintenance of the steady state for an extended operation over several hours. Additionally, the process indicated the potential for even longer process durations for most enzyme cascades. However, the reactor remains most effective for rapid synthesis reactions, and optimizing the enzyme cascades for maximal productivity is crucial. The developed reactor system has the potential to accommodate a broader range of nucleotide sugars.

Compared to single-batch processes commonly used for gram-scale nucleotide sugar production, the continuous fed-batch membrane reactor achieved similar productivities with a reduced biocatalyst load. Operating in a steady state through constant substrate feeding and product removal, the reactor benefits from optimal enzyme kinetics. Therefore, introducing new and more potent engineered enzymes with optimized kinetics shall be the next step for improved enzyme and reactor performance. In summary, continuous production represents a potent technology for established nucleotide sugar enzyme cascades.

## CRediT authorship contribution statement

**Nikol Kodra:** Methodology, Formal analysis, Data curation. **Hannes Frohnmeyer:** Writing – original draft, Visualization, Validation, Methodology, Investigation, Data curation, Conceptualization. **Lothar Elling:** Writing – review & editing, Validation, Supervision, Project administration, Methodology, Funding acquisition, Data curation.

## Declaration of Competing Interest

This work encompasses an industrial-driven project. All prepared nucleotide sugar solutions were sent to our industrial partner for product purification. The details of the purification procedures cannot be fully disclosed. The described production of nucleotide sugars in a continuous fed-batch membrane reactor is subject to a patent application.

## Data availability

Data will be made available on request.

## Acknowledgments

Financial support by the German Federal Ministry of Economic Affairs and Energy (BMWK) as part of the ZIM project: “Entwicklung einer enzymatischen Syntheseplattform ‘NukZuk’ für Nukleotidzucker und funktionalisierte Nukleotidzuckerderivate” (ZF4788501AJ9) is gratefully acknowledged. The authors thank Truc Pham and Dennis Hirtz for their valuable contributions.

## Appendix A. Supporting information

Supplementary data associated with this article can be found in the online version at doi:10.1016/j.jbiotec.2024.09.001.

## References

Bourgeaux, V., Piller, F., Piller, V., 2005. Two-step enzymatic synthesis of UDP-N-acetylgalactosamine. ACS Med. Chem. Lett. 15, 5459–5462. https://doi.org/10.1016/j.bmcl.2005.08.088.

Bülter, T., Elling, L., 2000. Enzymatic synthesis of UDP-galactose on a gram scale. J. Mol. Catal. B Enzym. 8, 281–284. https://doi.org/10.1016/S1381-1177(99)00079-X.

Bülter, T., Schumacher, T., Namdjou, D.J., Gutiérrez Gallego, R., Clausen, H., Elling, L., 2001. Chemoenzymatic synthesis of biotinylated nucleotide sugars as substrates for glycosyltransferases. Chembiochem 2, 884–894. https://doi.org/10.1002/1439-7633(20011203)2:12<884::Aid-cbic884>3.0.Co;2-2.

Bülter, T., Wandrey, C., Elling, L., 1997. Chemoenzymatic synthesis of UDP-N-acetyl-α-d-galactosamine. Carbohydr. Res. 305, 469–473. https://doi.org/10.1016/S0008-6215(97)10077-5.

Dias Gomes, M., Woodley, J.M., 2019. Considerations when Measuring Biocatalyst Performance. Mol 24, 3573. https://doi.org/10.3390/molecules24193573.

Eisele, A., Zaun, H., Kuballa, J., Elling, L., 2018. Cover Feature: In Vitro One-Pot Enzymatic Synthesis of Hyaluronic Acid from Sucrose and *N*-Acetylglucosamine: Optimization of the Enzyme Module System and Nucleotide Sugar Regeneration (ChemCatChem 14/2018). -2924 ChemCatChem 10, 2924. https://doi.org/10.1002/cctc.201801075.

Elling, L., Ritter, J.E., Verseck, S., 1996. Expression, purification and characterization of recombinant phosphomannomutase and GDP-alpha-D-mannose pyrophosphorylase from Salmonella enterica, group B, for the synthesis of GDP-alpha-D-mannose from D-mannose. J. Glycobiol. 6, 591–597. https://doi.org/10.1093/glycob/6.6.591.

Fey, S., Elling, L., Kragl, U., 1997. The cofactor $Mg^{2+}$—a key switch for effective continuous enzymatic production of GDP-mannose using recombinant GDP-mannose pyrophosphorylase. Carbohydr. Res. 305, 475–481. https://doi.org/10.1016/S0008-6215(97)10095-7.

Fischöder, T., Wahl, C., Zerhusen, C., Elling, L., 2019. Repetitive Batch Mode Facilitates Enzymatic Synthesis of the Nucleotide Sugars UDP-Gal, UDP-GlcNAc, and UDP-GalNAc on a Multi-Gram Scale. Biotechnol. J. 14 https://doi.org/10.1002/biot.201800386.

Frohnmeyer, H., Elling, L., 2023. Enzyme cascades for the synthesis of nucleotide sugars: Updates to recent production strategies. Carbohydr. Res. 523, 108727 https://doi.org/10.1016/j.carres.2022.108727.

Frohnmeyer, H., Rueben, S., Elling, L., 2022. Gram-Scale Production of GDP-β-L-fucose with Multi-Enzyme Cascades in a Repetitive-Batch Mode. ChemCatChem 14, e202200443. https://doi.org/10.1002/cctc.202200443.

Frohnmeyer, H., Verkade, J.M.M., Spiertz, M., Rentsch, A., Hoffmann, N., Sobota, M., Schwede, F., Tjeerdsma, P., Elling, L., 2024. Process Development for the Enzymatic Gram-Scale Production of the Unnatural Nucleotide Sugar UDP-6-azido-GalNAc. ChemSusChem, e202400311. https://doi.org/10.1002/cssc.202400311.

Gottschalk, J., Aßmann, M., Kuballa, J., Elling, L., 2022. Repetitive Synthesis of High-Molecular-Weight Hyaluronic Acid with Immobilized Enzyme Cascades. ChemSusChem 15, e202101071. https://doi.org/10.1002/cssc.202101071.

Gottschalk, J., Blaschke, L., Aßmann, M., Kuballa, J., Elling, L., 2021. Integration of a Nucleoside Triphosphate Regeneration System in the One-pot Synthesis of UDP-sugars and Hyaluronic Acid. ChemCatChem 13, 3074–3083. https://doi.org/10.1002/cctc.202100462.

Gottschalk, J., Zaun, H., Eisele, A., Kuballa, J., Elling, L., 2019. Key Factors for a One-Pot Enzyme Cascade Synthesis of High Molecular Weight Hyaluronic Acid. Int. J. Mol. Sci. 20, 5664. https://doi.org/10.3390/ijms20225664.

Gutmann, A., Nidetzky, B., 2016. Unlocking the Potential of Leloir Glycosyltransferases for Applied Biocatalysis: Efficient Synthesis of Uridine 5′-Diphosphate-Glucose by Sucrose Synthase. ASC 358, 3600–3609. https://doi.org/10.1002/adsc.201600754.

Hussnaetter, K.P., Palm, P., Pich, A., Franzreb, M., Rapp, E., Elling, L., 2023. Strategies for Automated Enzymatic Glycan Synthesis (AEGS). Biotechnol. Adv. 67, 108208 https://doi.org/10.1016/j.biotechadv.2023.108208.

Jeudy, S., Claverie, J.M., Abergel, C., 2006. The nucleoside diphosphate kinase from mimivirus: a peculiar affinity for deoxypyrimidine nucleotides. J. Bioenerg. Biomembr. 38, 247–254. https://doi.org/10.1007/s10863-006-9045-y.

Jeudy, S., Lartigue, A., Claverie, J.M., Abergel, C., 2009. Dissecting the unique nucleotide specificity of mimivirus nucleoside diphosphate kinase. J. Virol. 83, 7142–7150. https://doi.org/10.1128/jvi.00511-09.

Khodzhaieva, R.S., Gladkov, E.S., Kyrychenko, A., Roshal, A.D., 2021. Progress and Achievements in Glycosylation of Flavonoids. Front. Chem. 9, 637994 https://doi.org/10.3389/fchem.2021.637994.

Kragl, U., Klein, T., Vasic-Racki, D., Kittelmann, M., Ghisalba, O., Wandrey, C., 1996. Reaction engineering aspects of activated sugar production. CMP-Neu5Ac as an example. Ann. N. Y. Acad. Sci. 799, 577–583. https://doi.org/10.1111/j.1749-6632.1996.tb33260.x.

Kulmer, S.T., Gutmann, A., Lemmerer, M., Nidetzky, B., 2017. Biocatalytic Cascade of Polyphosphate Kinase and Sucrose Synthase for Synthesis of Nucleotide-Activated Derivatives of Glucose. Adv. Synth. Catal. 359, 292–301. https://doi.org/10.1002/adsc.201601078.

Lemmerer, M., Schmölzer, K., Gutmann, A., Nidetzky, B., 2016. Downstream Processing of Nucleoside-Diphospho-Sugars from Sucrose Synthase Reaction Mixtures at Decreased Solvent Consumption. ASC 358, 3113–3122. https://doi.org/10.1002/adsc.201600540.

Li, C., Wang, L.X., 2018. Chemoenzymatic methods for the synthesis of glycoproteins. Chem. Rev. 118, 8359–8413. https://doi.org/10.1021/acs.chemrev.8b00238.

Li, L., Liu, Y., Wan, Y., Li, Y., Chen, X., Zhao, W., Wang, P.G., 2013. Efficient Enzymatic Synthesis of Guanosine 5′-Diphosphate-Sugars and Derivatives. Org. Lett. 15, 5528–5530. https://doi.org/10.1021/ol402585c.

Li, S., Wang, S., Wang, Y., Qu, J., Liu, X.-w, Wang, P.G., Fang, J., 2021. Gram-scale production of sugar nucleotides and their derivatives. Green. Chem. 23, 2628–2633. https://doi.org/10.1039/D1GC00711D.

Liu, H., Tegl, G., Nidetzky, B., 2021. Glycosyltransferase Co-Immobilization for Natural Product Glycosylation: Cascade Biosynthesis of the C-Glucoside Nothofagin with Efficient Reuse of Enzymes. ASC 363, 2157–2169. https://doi.org/10.1002/adsc.202001549.

Mahour, R., Lee, J.W., Grimpe, P., Boecker, S., Grote, V., Klamt, S., Seidel-Morgenstern, A., Rexer, T.F.T., Reichl, U., 2022. Cell-free multi-enzyme synthesis and purification of uridine diphosphate galactose. ChemBioChem 23, e202100361. https://doi.org/10.1002/cbic.202100361.

Mahour, R., Marichal-Gallardo, P.A., Rexer, T.F.T., Reichl, U., 2021. Multi-enzyme Cascades for the In Vitro Synthesis of Guanosine Diphosphate L-Fucose. ChemCatChem 13, 1981–1989. https://doi.org/10.1002/cctc.202001854.

Mikkola, S., 2020. Nucleotide Sugars in Chemistry and Biology. Mol 25. https://doi.org/10.3390/molecules25235755.

Nishimoto, M., Kitaoka, M., 2007. Identification of N-Acetylhexosamine 1-Kinase in the Complete Lacto-N-Biose I/Galacto-N-Biose Metabolic Pathway in Bifidobacterium longum. AEM 73, 6444–6449. https://doi.org/10.1128/AEM.01425-07.

Ohashi, H., Wahl, C., Ohashi, T., Elling, L., Fujiyama, K., 2017. Effective Synthesis of Guanosine 5′-Diphospho-β-l-galactose Using Bacterial l-Fucokinase/Guanosine 5′-Diphosphate-l-fucose Pyrophosphorylase. ASC 359, 4227–4234. https://doi.org/10.1002/adsc.201700901.

Orrego, A.H., Trobo-Maseda, L., Rocha-Martin, J., Guisan, J.M., 2017. Immobilization-stabilization of a complex multimeric sucrose synthase from Nitrosomonas europaea. Synthesis of UDP-glucose. Enzym. Micro Technol. 105, 51–58. https://doi.org/10.1016/j.enzmictec.2017.06.008.

Petschacher, B., Nidetzky, B., 2016. Biotechnological production of fucosylated human milk oligosaccharides: Prokaryotic fucosyltransferases and their use in biocatalytic cascades or whole cell conversion systems. J. Biotech. 235, 61–83. https://doi.org/10.1016/j.jbiotec.2016.03.052.

Pollard, D.J., Woodley, J.M., 2007. Biocatalysis for pharmaceutical intermediates: the future is now. Trends Biotechnol. 25, 66–73. https://doi.org/10.1016/j.tibtech.2006.12.005.

Rexer, T., Laaf, D., Gottschalk, J., Frohnmeyer, H., Rapp, E., Elling, L., 2021. Enzymatic Synthesis of Glycans and Glycoconjugates. Adv. Biochem. Engin. /Biotechnol. 231–280. https://doi.org/10.1007/10_2020_148.

Rexer, T.F.T., Schildbach, A., Klapproth, J., Schierhorn, A., Mahour, R., Pietzsch, M., Rapp, E., Reichl, U., 2018. One pot synthesis of GDP-mannose by a multi-enzyme cascade for enzymatic assembly of lipid-linked oligosaccharides. Biotechnol. Bioeng. 115, 192–205. https://doi.org/10.1002/bit.26454.

Song, J., Zhang, H., Wu, B., Zhang, Y., Li, H., Xiao, M., Wang, P.G., 2003. Reassembled Biosynthetic Pathway for a Large-scale Synthesis of CMP-Neu5Ac. Mar. Drugs 1, 34–45.

Wagner, G.K., Pesnot, T., Field, R.A., 2009. A survey of chemical methods for sugar-nucleotide synthesis. Nat. Prod. Rep. 26, 1172–1194. https://doi.org/10.1039/B909621N.

Wahl, C., Hirtz, D., Elling, L., 2016. Multiplexed Capillary Electrophoresis as Analytical Tool for Fast Optimization of Multi-Enzyme Cascade Reactions – Synthesis of Nucleotide Sugars. Biotechnol. J. 11, 1298–1308. https://doi.org/10.1002/biot.201600265.

Wahl, C., Spiertz, M., Elling, L., 2017. Characterization of a new UDP-sugar pyrophosphorylase from Hordeum vulgare (barley). Biotechnol. J. 258, 51–55. https://doi.org/10.1016/j.jbiotec.2017.03.025.

Walsh, C., Lane, J.A., van Sinderen, D., Hickey, R.M., 2020. From lab bench to formulated ingredient: Characterization, production, and commercialization of human milk oligosaccharides. J. Funct. Foods 72, 104052. https://doi.org/10.1016/j.jff.2020.104052.

Wang, L.X., Lomino, J.V., 2012. Emerging technologies for making glycan-defined glycoproteins. ACS Chem. Biol. 7, 110–122. https://doi.org/10.1021/cb200429n.

Wang, S., Zhang, J., Wei, F., Li, W., Wen, L., 2022. Facile Synthesis of Sugar Nucleotides from Common Sugars by the Cascade Conversion Strategy. J. Am. Chem. Soc. 144, 9980–9989. https://doi.org/10.1021/jacs.2c03138.

Wijdeven, M.A., van Geel, R., Hoogenboom, J.H., Verkade, J.M.M., Janssen, B.M.G., Hurkmans, I., de Bever, L., van Berkel, S.S., van Delft, F.L., 2022. Enzymatic glycan remodeling-metal free click (GlycoConnect™) provides homogenous antibody-drug conjugates with improved stability and therapeutic index without sequence engineering. MAbs 14, 2078466. https://doi.org/10.1080/19420862.2022.2078466.

Wu, S., Snajdrova, R., Moore, J.C., Baldenius, K., Bornscheuer, U.T., 2021. Biocatalysis: Enzymatic Synthesis for Industrial Applications. Angew. Chem., Int. Ed. 60, 88–119. https://doi.org/10.1002/anie.202006648.

Zhao, G., Guan, W., Cai, L., Wang, P.G., 2010. Enzymatic route to preparative-scale synthesis of UDP–GlcNAc/GalNAc, their analogues and GDP–fucose. Nat. Protoc. 5, 636–646. https://doi.org/10.1038/nprot.2010.3.

Zou, Y., Xue, M., Wang, W., Cai, L., Chen, L., Liu, J., Wang, P.G., Shen, J., Chen, M., 2013. One-pot three-enzyme synthesis of UDP-Glc, UDP-Gal, and their derivatives. Carbohydr. Res. 373, 76–81. https://doi.org/10.1016/j.carres.2013.03.005.